Fully interferometric controllable anomalous refraction efficiency using cross modulation with plasmonic metasurfaces

Zhaocheng Liu,[1] Shuqi Chen,[1,*] Jianxiong Li,[1] Hua Cheng,[1] Zhancheng Li,[1] Wenwei Liu,[1] Ping Yu,[1] Ji Xia,[1] and Jianguo Tian[1,2]

[1]*Key Laboratory of Weak Light Nonlinear Photonics, Ministry of Education, School of Physics and Teda Applied Physics Institute, Nankai University, Tianjin 300071, China*

[2]*e-mail: jjtian@nankai.edu.cn*

**Corresponding author: schen@nankai.edu.cn*

Received September 10, 2014; revised October 21, 2014; accepted October 29, 2014; posted October 30, 2014 (Doc. ID 222814); published December 1, 2014

We present a method of fully interferometric, controllable anomalous refraction efficiency by introducing cross-modulated incident light based on plasmonic metasurfaces. Theoretical analyses and numerical simulations indicate that the anomalous and ordinary refracted beams generated from two opposite-helicity incident beams and following the generalized Snell's law will have a superposition for certain incident angles, and the anomalous refraction efficiency can be dynamically controlled by changing the relative phase of the incident sources. As the incident wavelength nears the resonant wavelength of the plasmonic metasurfaces, two equal-amplitude incident beams with opposite helicity can be used to control the anomalous refraction efficiency. Otherwise, two unequal-amplitude incident beams with opposite helicity can be used to fully control the anomalous refraction efficiency. This Letter may offer a further step in the development of controllable anomalous refraction.

OCIS codes: (160.3918) Metamaterials; (240.6680) Surface plasmons; (230.4555) Coupled resonators.
http://dx.doi.org/10.1364/OL.39.006763

Metasurfaces, a new class of metamaterials that consist of a monolayer of planar metallic structures, have shown great promise for generating a wide range of position-dependent, discontinuous interfacial phase profiles [1,2]. By simply engineering a metasurface-induced phase profile, a nearly arbitrary wavefront can be produced. The field of metasurfaces is rapidly expanding, with applications such as anomalous refraction [1,3], optical vortex beams [4,5], aberration-free quarter-wave plates [6], ultra-thin flat lenses [7,8], optical spin–orbital interactions [9,10], and high-resolution, three-dimensional metasurface holograms [11,12]. The realization of anomalous refraction through linear control of phase discontinuity is a common goal with these applications, although most have only achieved it for the orthogonal portion of incident polarization, which leaves both of the anomalous and ordinary refractions. Therefore, the limited efficiency of polarization conversion results in low anomalous refraction efficiency. Recently, [13] presented ultrathin broadband polarization converters capable of rotating a linear polarization state into its orthogonal one. On the basis of these converters, the anomalous refraction efficiency can be markedly increased, although this method still needs further improvement in some applications. A type of cascaded metasurface was proposed in [14], which uses collocated electric and magnetic polarizabilities to induce low polarization and reflection loss, leading to high-efficiency anomalous refraction. This kind of metasurface relies on a multilayer nanostructure, requiring complex sample fabrication and critical alignment between layers. Moreover, the anomalous refraction efficiency in [13,14] still cannot be fully controlled, which extremely limits the development of controllable anomalous refraction.

In this Letter, we propose a novel method of fully interferometric, controllable anomalous refraction efficiency, by incorporating cross-modulated incident light with plasmonic metasurfaces. We demonstrate, theoretically and numerically, that the anomalous and ordinary refracted light generated by two opposite-helicity incident beams will have a superposition for certain incident angles, and the anomalous refraction efficiency can be dynamically controlled by changing their relative phase. As the incident wavelength and resonant wavelength of the metasurface converge, two equal-amplitude incident beams with opposite helicity can finely control the anomalous refraction efficiency. Otherwise, we need to adopt two unequal-amplitude incident beams with opposite helicity for comprehensive controlling.

Figure 1(a) shows a plasmonic metasurface capable of generating ordinary and anomalous refraction with opposite circular polarization. This metasurface consists of arrays of identically shaped gold nanorods (length $l = 300$ nm, width $w = 50$ nm, and thickness $t = 50$ nm), which exhibit a resonance at a wavelength of 1.3 μm, and are arranged evenly along the x-direction, with the orientation angle increasing in 22.5° increments. The length and width of the unit cell, indicated by a white rectangle in Fig. 1(a), are $L = 3800$ nm and $W = 475$ nm, respectively. The optical constants of gold are $\varepsilon = -67.9 + 6.65i$ at 1.3 μm and $\varepsilon = -62.8 + 4.96i$ at 1.15 μm [15]; the permittivity of the substrate is taken as 2.25. All numerical simulations were carried out using finite-element method (FEM)-based commercial software, COMSOL Multiphysics [16].

A nanorod antenna will absorb and scatter some fraction of the incident light, and transmit the incident light of any polarization; thus, it can be treated as an imperfect linear polarizer, with polarization directions indicated by the green arrows in Fig. 1(a). According to the Jones matrix, perfect polarizers with rotation angle φ can be described as

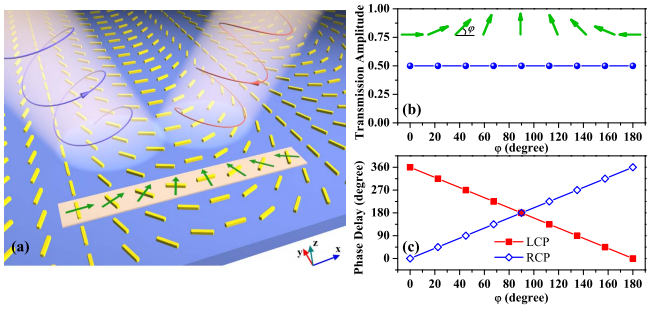

Fig. 1. (a) Schematic illustration of a representative plasmonic metasurface used as a model in our theory and simulation. (b) Amplitude transmission of anomalous light scattered from each linear polarizer as a function of rotation angle φ when $\beta = 0.5$. (c) Phase delay of anomalous light scattered from each linear polarizer as a function of rotation angle φ.

$$P = \begin{bmatrix} \cos^2\varphi & \sin\varphi\cos\varphi \\ \sin\varphi\cos\varphi & \sin^2\varphi \end{bmatrix}, \tag{1}$$

where φ is a linear function of x and can be specified as $\varphi(x) = \pi x/L$. A circularly polarized (CP) beam is primarily scattered into waves of the same polarization as that of the incident beam without phase change, and partially converted into the opposite-handedness of CP light, with phase change [5,17,18]. We adopt the Dirac bracket notation to define right-circularly polarized (RCP) and left-circularly polarized (LCP) waves as $|R\rangle = [1 \quad i]^{\mathrm{T}}$ and $|L\rangle = [1 \quad -i]^{\mathrm{T}}$, respectively. The linearly polarized light generated by the polarizer can be seen as the combination of two CP beams with opposite helicity. Therefore, the transmission process for the gold nanorod arrays can be written as

$$P|L\rangle = \alpha|L\rangle + \beta|R\rangle e^{-i2\varphi}, \tag{2}$$

$$P|R\rangle = \alpha|R\rangle + \beta|L\rangle e^{i2\varphi}, \tag{3}$$

where α and β are the amplitude of the refracted beams and maintain $\alpha + \beta = 1$ after normalization; the phase factor $e^{\pm i2\varphi}$ indicates an abrupt phase change imposed on anomalous beams. The transmission amplitude of the anomalous beam is shown in Fig. 1(b), where both linear polarizers can refract light with the converted helicity of incidence. Obviously, a linear polarizer can exhibit perfect polarization behavior when the amplitude conversion efficiency β of the polarization array is 0.5. Figure 1(c) shows the phase delay of an anomalous beam, scattered from each linear polarizer. When a polarizer has a linear rotation along the x-axis from 0 to π, eight linear polarizers can cover the entire phase range of 0 to 2π; this phase change is opposite for LCP and RCP incident beams.

An arbitrary incident state $|\psi\rangle = c_1|L\rangle + c_2|R\rangle$ can be achieved by combining LCP and RCP, where c_1 and c_2 are complex numbers. Substituting this polarization state into the eigenvalue equation $P|\psi\rangle = p|\psi\rangle$ (where p is the eigenvalue), we can obtain two groups of eigenvalues and eigenstates as follows:

$$p_1 = \alpha + \beta \quad \text{and} \quad |\psi_1\rangle = e^{i\varphi}|L\rangle + e^{-i\varphi}|R\rangle, \tag{4}$$

$$p_2 = \alpha - \beta \quad \text{and} \quad |\psi_2\rangle = e^{i\varphi}|L\rangle - e^{-i\varphi}|R\rangle. \tag{5}$$

Thus, only two refractive beams with opposite helicity are present in the transmitted beams, even for different amplitudes (p_1 and p_2). The eigenstates in Eqs. (4) and (5) have the same phase factor, apart from the phase shift π for $|R\rangle$. The spatial frequencies of the LCP and RCP beams can be written as $u_L = \sin\theta_L/\lambda$ and $u_R = \sin\theta_R/\lambda$, where θ_L and θ_R are incident angles for the LCP and RCP incident beams. Then, the phase factor of LCP light can be written as $c_1 = e^{i2\pi u_L x}$. The relation $c_2 = \pm c_1 e^{-i2\varphi}$, deduced from Eqs. (4) and (5), can be Fourier transformed:

$$F\{c_2\} = \delta\left[u_R - \left(u_L - \frac{1}{L}\right)\right]. \tag{6}$$

Therefore, the relation between two incident angles meeting the eigenstates can be written as

$$\sin\theta_R = \sin\theta_L - \frac{\lambda_0}{n_1 L}, \tag{7}$$

where λ_0 is the wavelength in free space, and n_1 is the refractive index for the incident side. If θ_L and θ_R satisfy Eq. (7), the anomalous and ordinary refracted beams for both LCP and RCP incident beams will have a superposition, and vice versa, as shown in Fig. 2(a). Figure 2(b) shows the calculated LCP incident angle θ_L as a function of the RCP incident angle θ_R. The incident angles are restricted by evanescence and total reflection, so LCP and RCP incident angles are limited to –26.0°–41.8° and –41.8°–26.0°, respectively. To simplify our analysis, we will choose two symmetric incident angles, $\theta_L = -\theta_R = 6.5°$, for the following discussion. The reflected beams will superpose with two incident beams, so we do not discuss this case.

As the anomalous and ordinary refracted beams are superposable and interactional, the efficiency of anomalous refraction can be controlled by changing the relative phase Φ of the incident beams. An arbitrary incident state

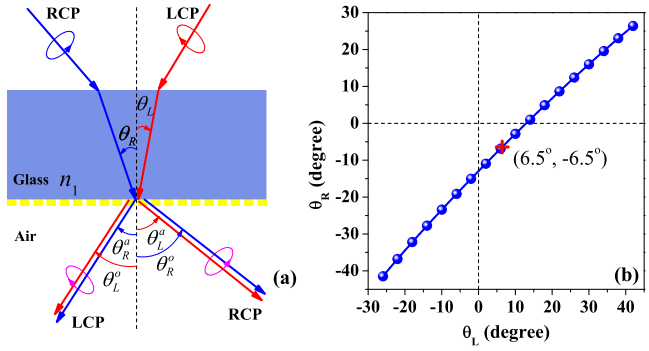

Fig. 2. (a) Schematic illustration of the anomalous and ordinary refracted lights for both LCP and RCP incident beams, which are superposable at all eigenstates. (b) Calculated LCP incident angle θ_L as a function of the RCP incident angle θ_R. Red marker shows two symmetric incident angles, $\theta_L = -\theta_R = 6.5°$.

can be written as $|\psi\rangle = e^{i\varphi}|L\rangle + e^{-i(\varphi-\Phi)}|R\rangle$, where the LCP and RCP incident beams have equal amplitude. Sending the arbitrary incident light through the polarization arrays, we can produce the transmitted light from Eqs. (2) and (3):

$$P|\psi\rangle = (\alpha + \beta e^{i\Phi})e^{i\varphi}|L\rangle + (\alpha e^{i\Phi} + \beta)e^{-i\varphi}|R\rangle. \quad (8)$$

Apparently, the amplitude for two refracted beams with opposite helicity is $|E_L| = |E_R| = \sqrt{\alpha^2 + \beta^2 + 2\alpha\beta\cos\Phi}$. The maximal amplitude $|E_{\max}|$ and minimal amplitude $|E_{\min}|$ correspond to the eigenvalues in Eqs. (4) and (5), respectively, when $\Phi = 0$ and $\Phi = \pi$. We accordingly defined the degree of modulation (DOM) $\eta = 1 - |E_{\min}|^2/|E_{\max}|^2$ to evaluate the controllability of transmitted beams for the polarization arrays. The calculated η with varying conversion efficiency β is shown in Fig. 3(a). We can see that η reaches its maximum when $\beta = 0.5$, and its value gradually decreases as β deviates from 0.5.

Full three-dimensional simulations were performed to demonstrate our theory. Two opposite-helicity incident beams with equal-amplitude were set. We fixed the RCP beam, gradually tuned the phase of the LCP beam, and then detected the intensity of refracted light for the RCP beam. The red marker in Fig. 3(a) shows the values of $\beta = 0.38$ and $\eta = 0.94$ at the resonant wavelength of 1.3 μm for the proposed metasurface. Figure 3(b) gives the calculated and simulated intensity $|E_R|^2$ of the RCP transmitted light for different relative phases Φ when $\beta = 0.38$ and $\beta = 0.5$. When $\Phi = 0$, the intensity $|E_R|^2$ of the RCP transmitted light reaches its maximum; it then decreases as Φ increases and reaches its minimum when $\Phi = \pi$. Thus, the controllable process is periodic with increasing Φ. The simulated results (blue circles) are in good agreement with our theoretical results (solid red line) for the case of $\beta = 0.38$. The theoretical results for $\beta = 0.5$ correspond to perfectly controllable refracted light. Therefore, the RCP anomalous refracted light can be controlled by changing the relative phase of the RCP and LCP incident lights. The ordinary and anomalous diffractions are small in our case, so we did not discuss them [19]. However, it is an interesting issue to control the intensity of the diffracted lights using our method.

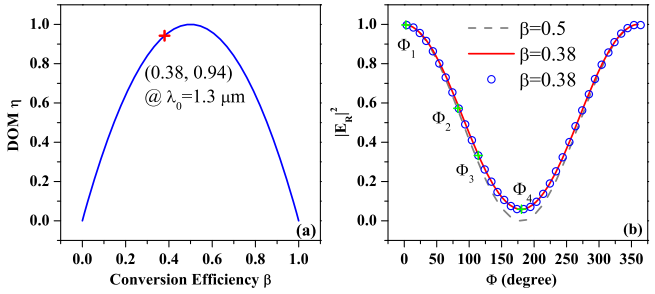

Fig. 3. (a) Calculated DOM η with varying the conversion efficiency β. Red marker shows the values of $\beta = 0.38$ and $\eta = 0.94$ at the resonant wavelength of 1.3 μm. (b) Calculated (dashed gray line and solid red line) and simulated (blue circles) intensity $|E_R|^2$ of the RCP transmitted light for varying relative phase Φ when $\beta = 0.38$ and $\eta = 0.94$.

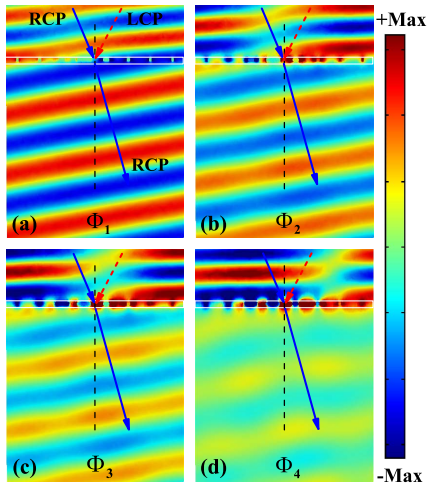

Fig. 4. Simulated electric field distributions of RCP refracted light at different relative phases, which are indicated by green markers in Fig. 3(b): (a) $\Phi_1 = 0°$, (b) $\Phi_2 = 82°$, (c) $\Phi_3 = 115°$, and (d) $\Phi_4 = 180°$.

Figure 4 shows the simulated electric field distributions of RCP refracted light at different relative phases Φ, which have been indicated by green markers in Fig. 3(b). When $\Phi = 0$, the wavefront and amplitude of the RCP refracted light are distinct and maximal, as shown in Fig. 4(a). With increasing Φ, the RCP refracted light gradually becomes weak and nearly disappears, as can be seen in Figs. 4(b)–4(c). These characteristics are consistent with the results from Fig. 3(b).

When the incident wavelength is far away from the resonant wavelength of metasurface, the conversion efficiency will gradually decrease. The anomalous refraction efficiency cannot be efficiently controlled anymore by two equal-amplitude incident beams with opposite helicity. We can adopt two unequal-amplitude incident beams with opposite helicity to fully control the anomalous refraction efficiency. We defined an arbitrary incident state with unequal amplitude for the LCP and RCP incident beams as $|\psi\rangle = ae^{i\varphi}|L\rangle + be^{-i(\varphi-\Phi)}|R\rangle$. As mentioned previously, the amplitudes of the LCP and RCP refracted beams $|E_{L,R}| = \sqrt{\alpha_{L,R}^2 + \beta_{L,R}^2 + 2\alpha_{L,R}\beta_{L,R}\cos\Phi}$ can be deduced, where $\alpha_L = a\alpha$, $\beta_L = b\beta$, $\alpha_R = a\beta$, and $\beta_R = b\alpha$. In this Letter, $\beta_{L,R}$ can be treated as the effective conversion efficiency for the LCP and RCP beams, which can separately produce perfectly controllable anomalous refracted light by setting the amplitude ratios $a/b = \beta/\alpha$ and $a/b = \alpha/\beta$ for $\beta_L = 0.5$ and $\beta_R = 0.5$, respectively. Next, we will discuss the case where $\beta = 0.28$, which corresponds to an incident wavelength of 1.15 μm.

Figure 5 shows the calculated and simulated intensity $|E_R|^2$ of the RCP transmitted light as a function of relative phase Φ for two cases of the amplitude ratio a/b when $\beta = 0.28$. We can see that the RCP anomalous refracted light cannot be fully controlled in the case where $a/b = 1$, and η is 0.8 for the incident beams with equal amplitude. However, when the amplitude ratio $a/b = 2.57$, η goes to 1.0, and it is clear that the RCP anomalous refracted light is fully controllable. The simulated results (blue circles) are also in good agreement with our proposed theoretical results (solid red line)

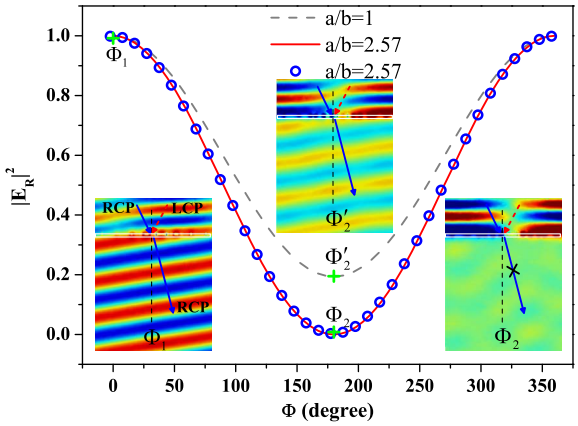

Fig. 5. Calculated (dashed gray line and solid red line) and simulated (blue circles) intensity $|E_R|^2$ of the RCP transmitted light as a function of relative phase Φ for different amplitude ratios a/b when $\beta = 0.28$. Insets: simulated electric field distributions of RCP refracted light at the relative phases $\Phi_1 = 0°$ and $\Phi_2 = \Phi'_2 = 180°$ for the equal and unequal amplitude cases, respectively.

for the unequal-amplitude case. The electric field distributions (insets of Fig. 5) further confirm these assertions.

In conclusion, we have demonstrated a novel method of fully controllable, anomalous refraction efficiency via cross-modulated, opposite-helicity incident light, with plasmonic metasurfaces. When two opposite-helicity incident beams have equal amplitude, the DOM mostly depends on the conversion efficiency. Otherwise, the DOM and effective conversion efficiency can reach ideal values by setting suitable amplitude-ratio, opposite-helicity incident beams. The anomalous refraction efficiency can also be dynamically controlled by changing the relative phase of incident beams (i.e., adjusting the optical path difference). Our Letter thus provides a promising method for fully controllable, anomalous refraction that may extend to other applications, such as vortex beams, flat lenses, metasurface holograms, and so on.

This Letter was supported by the National Basic Research Program (973 Program) of China (2012CB921900), Chinese National Key Basic Research Special Fund (2011CB922003), Natural Science Foundation of China (61378006 and 11304163), Program for New Century Excellent Talents in University (NCET-13-0294), Natural Science Foundation of Tianjin (13JCQNJC01900), National Science Fund for Talent Training in Basic Sciences (J1103208), and the 111 project (B07013).

References

1. N. Yu, P. Genevet, M. A. Kats, F. Aieta, J. P. Tetienne, F. Capasso, and Z. Gaburro, Science **334**, 333 (2011).
2. N. Yu and F. Capasso, Nat. Mater. **13**, 139 (2014).
3. X. Ni, N. K. Emani, A. V. Kildishev, A. Boltasseva, and V. M. Shalaev, Science **335**, 427 (2012).
4. P. Genevet, N. Yu, F. Aieta, J. Lin, M. A. Kats, R. Blanchard, M. O. Scully, Z. Gaburro, and F. Capasso, Appl. Phys. Lett. **100**, 013101 (2012).
5. L. Huang, X. Chen, H. Mühlenbernd, G. Li, B. Bai, Q. Tan, G. Jin, T. Zentgraf, and S. Zhang, Nano Lett. **12**, 5750 (2012).
6. N. Yu, F. Aieta, P. Genevet, M. A. Kats, Z. Gaburro, and F. Capasso, Nano Lett. **12**, 6328 (2012).
7. F. Aieta, P. Genevet, M. A. Kats, N. Yu, R. Blanchard, Z. Gaburro, and F. Capasso, Nano Lett. **12**, 4932 (2012).
8. X. Chen, L. Huang, H. Mhlenbernd, G. Li, B. Bai, Q. Tan, G. Jin, C. W. Qiu, S. Zhang, and T. Zentgraf, Nat. Commun. **3**, 1198 (2012).
9. X. Yin, Z. Ye, J. Rho, Y. Wang, and X. Zhang, Science **339**, 1405 (2013).
10. N. Shitrit, L. Yulevich, E. Maguid, D. Ozeri, D. Veksler, V. Kleiner, and E. Hasman, Science **340**, 724 (2013).
11. L. Huang, X. Chen, H. Mhlenbernd, H. Zhang, S. Chen, B. Bai, Q. Tan, G. Jin, K. W. Cheah, C. W. Qiu, J. Li, T. Zentgraf, and S. Zhang, Nat. Commun. **4**, 2808 (2013).
12. X. Ni, A. V. Kildishev, and V. M. Shalaev, Nat. Commun. **4**, 2807 (2013).
13. N. K. Grady, J. E. Heyes, D. R. Chowdhury, Y. Zeng, M. T. Reiten, A. K. Azad, A. J. Taylor, D. A. R. Dalvit, and H. T. Chen, Science **340**, 1304 (2013).
14. C. Pfeiffer and A. Gribc, Appl. Phys. Lett. **102**, 231116 (2013).
15. E. D. Palik, *Handbooks of Optical Constants of Solids* (Academic, 1998).
16. *COMSOL Multiphysics Users Guide*, Version 4.3 (COMSOL AB, 2012).
17. F. Gori, Opt. Lett. **24**, 584 (1999).
18. E. Hasman, Z. Bomzon, A. Niv, G. Biener, and V. Kleiner, Opt. Commun. **209**, 45 (2002).
19. L. Huang, X. Chen, B. Bai, Q. Tan, G. Jin, T. Zentgraf, and S. Zhang, Light Sci. Appl. **2**, e70 (2013).